Investigation of Programmable Automation Controller for AMB applications

Adam Krzysztof PILAT [a], Jakub KLOCEK [b]

[a] AGH University of Science and Technology, Faculty of Electrical Engineering, Automatics, Computer Science and Biomedical Engineering , Department of Automatic Control and Robotics
Mickiewicza 30, 30-059 Krakow, Poland
ap@agh.edu.pl
[b] OPTISTER, Krakow, Poland

***Abstract*—This article presents a results of selected hardware investigation done using the Programmable Automation Controller (PAC), The Device was placed at the laboratory test rig consisting of programmable devices: signal generator, oscilloscope, load. The controller was tested with respect to the requirements of active levitation devices. The analog power actuator was investigated and results are given in a form of plot diagrams.**

I. Active magnetic Bearings Controllers

The flexibility of configuration and implementation of control tasks means that more and more advanced methods and apparatus are used. ALM systems have been developed for decades, and technological progress in the field of electronics results in solutions in the form of various configurations of these mechatronic devices. It was digital solutions and the development of algorithms that enabled the implementation of complex dynamics control systems of machines using active magnetic levitation [2, 5, 6, 11, 13, 22, 23, 24, 26]). It should be remembered that in the first phase of research on magnetic levitation systems, they were controlled by means of analogue solutions [13], [15]. Reviewing various architectures of electromagnetic driver control systems [3, 9, 10, 13, 20] and other ALM systems [1, 4, 7, 12, 14, 21]), and referring to the works presented at conferences and symposia (including ISMB - International Symposium on Magnetic Bearings since 1988), three basic configurations can be distinguished:

- signal processors - DSP (Digital Signal Processor) used as autonomous or compact controllers manufactured by dSPACE,
- microcontrollers and general-purpose computer systems with integrated control and measurement cards,
- FPGA (Field Programmable Gate Arrays) systems used alone or cooperating with the above-mentioned architectures.

Depending on the equipment used, performance due to real-time control varies. In the literature one can find solutions using the dSPACE platform to control magnetic bearings with a sampling rate of 20 ÷ 40 kHz, microprocessor systems within 1 ÷ 2 kHz, signal processors of about 17.5 kHz and FPGA circuits of about 28 kHz.

II. Programmable Automation Controller

With respect to the high requirements set by the active magnetic levitation systems the developed platform was designed in such a way that it is possible to use it for monitoring and control applications of various devices and technological processes. The signal and data buses allow for a free transfer of analog and digital signals between particular modules. The signals are processed by programmable analog and digital devices as well [16, 17].

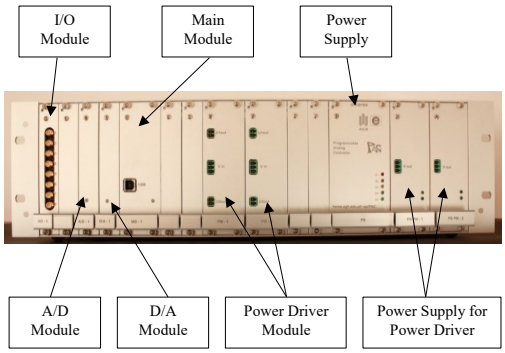

Figure 1. Programmable Automation Controller in the industrial chasis..

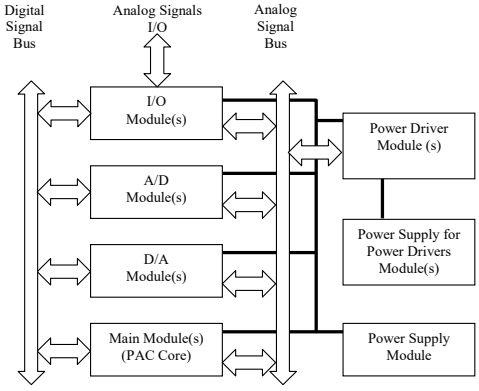

Figure 2. PAC Architecture.

The PAC architecture is similar to the digital multicore and multi processor computer. Modules are equipped with

individual processing units for dedicated tasks. The internal digital communication protocols and analog signal exchange allows to configure the functionality of the pAC on demand. A few PACs can be connected by the I/O modules exchanging analog signals in both directions, therefore they can be configured in a stack-able form to extend the functionality and peripherals.

III. Hardware Testing

From the practical applications point of view, the signal processing path characteristics is requested to be known. The laboratory test-rig was set-up using the following devices: signal generator (RIGOL DG4062), oscilloscope (RIGOL DS1054Z) and programmable load (RIGOL DL3031A).

This elaboration evaluates the performance of I/O and analog power module with respect to the sine, ramp, and square wave type input signals. The input signal frequencies were set as follows: 100Hz, 500Hz, 1kHz, 5kHz, 10kHz, 20kHz, 40kHz. The goal of planned research is to check the operation of commercial power amplifier.

The time diagrams are presented to show the response of the analog power module. Gain, offset, phase shift and signal distortions are well visible. The conducted research has shown static and dynamic properties of the device. Zaobserwowane zniekształcenia uniemożliwiają opracowanie charakterystyk Bodego. Dlatego też analiza sprowadza się do ogólnej oceny sygnałów.

IV. Identification without Load

The presented test results include analysis of voltage signals whose sources are: signal generator and output from the PAC controller's analog power system. The signal from the generator was applied to the analog input of the controller and then sent directly to the power module input. The full signal processing path is tested. Input and output voltages are analyzed.

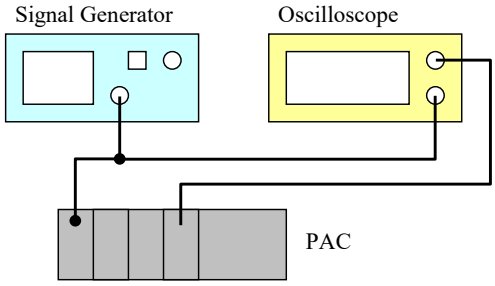

Figure 3. Schematic diagram of connections for Investigation of PAC.

In the open control loop system, good operation of the device up to 10kHz is observed (see Figs. 4÷6). Above this frequency, distortions are visible. This is related to the insufficient feedback configured at the power amplifier. In further work, it is necessary to modify the hardware layer to expand the bandwidth. Due to the occurring oscillations in the case of a rectangular signal, one can consider the new configuration of the power stage to obtain an aperiodic response with a configurable time constant. One can consider the option of implementing the current feedback in the power driver.

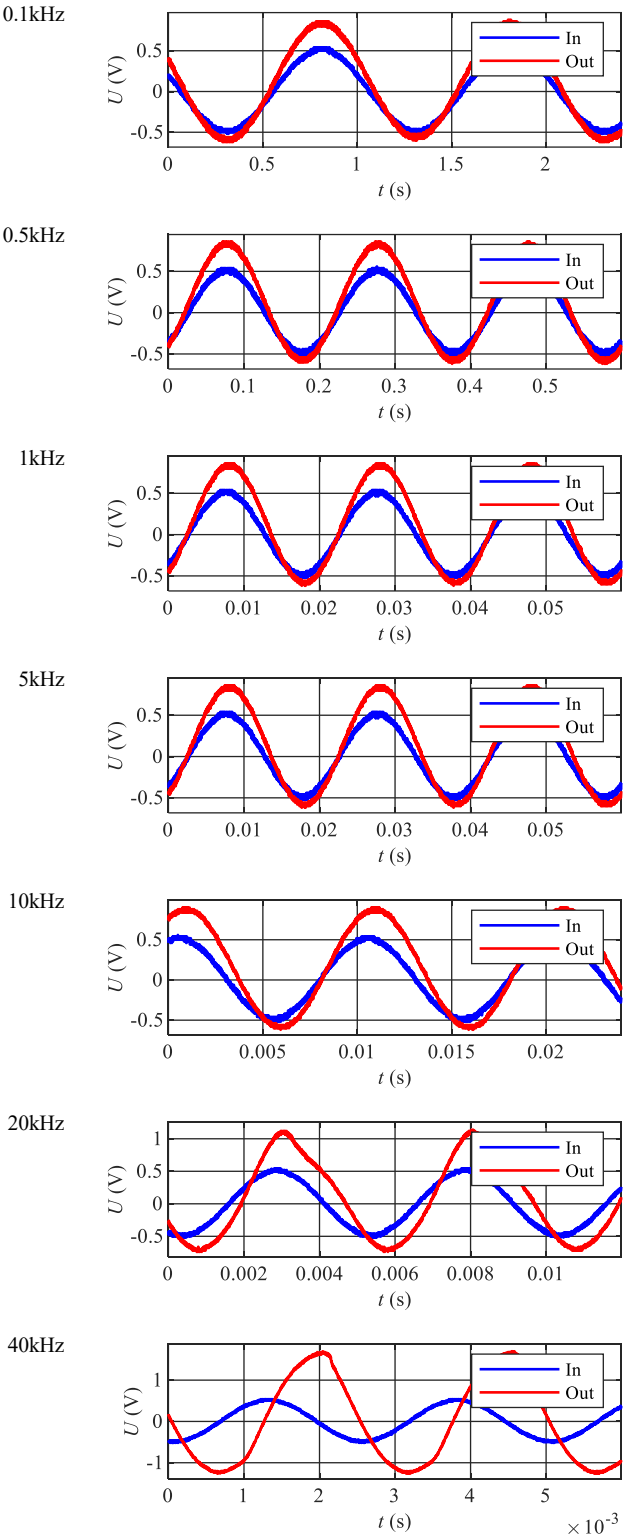

Figure 4. Measured power driver output without load with response to sine wve input in a range of 100Hz to 40kHz.at

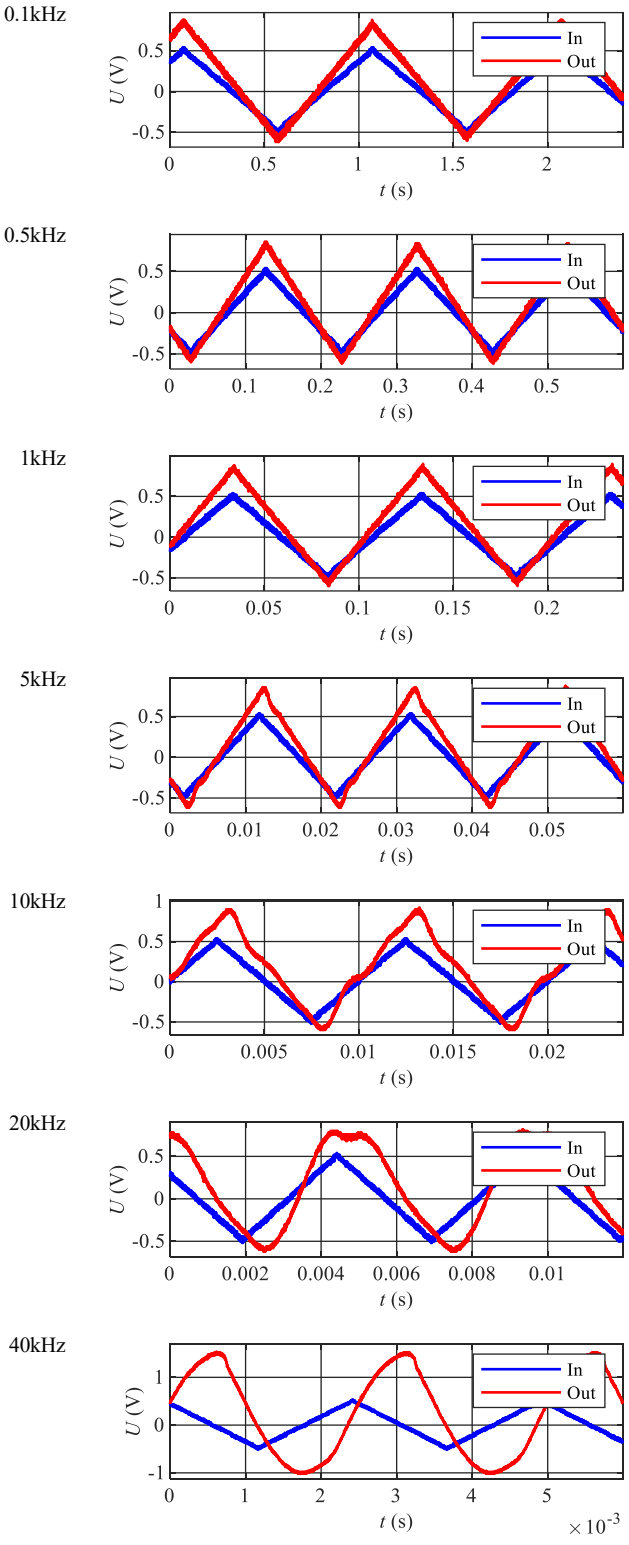

Figure 5. Measured power driver output without load with response to ramp wave input in a range of 100Hz to 40kHz.at

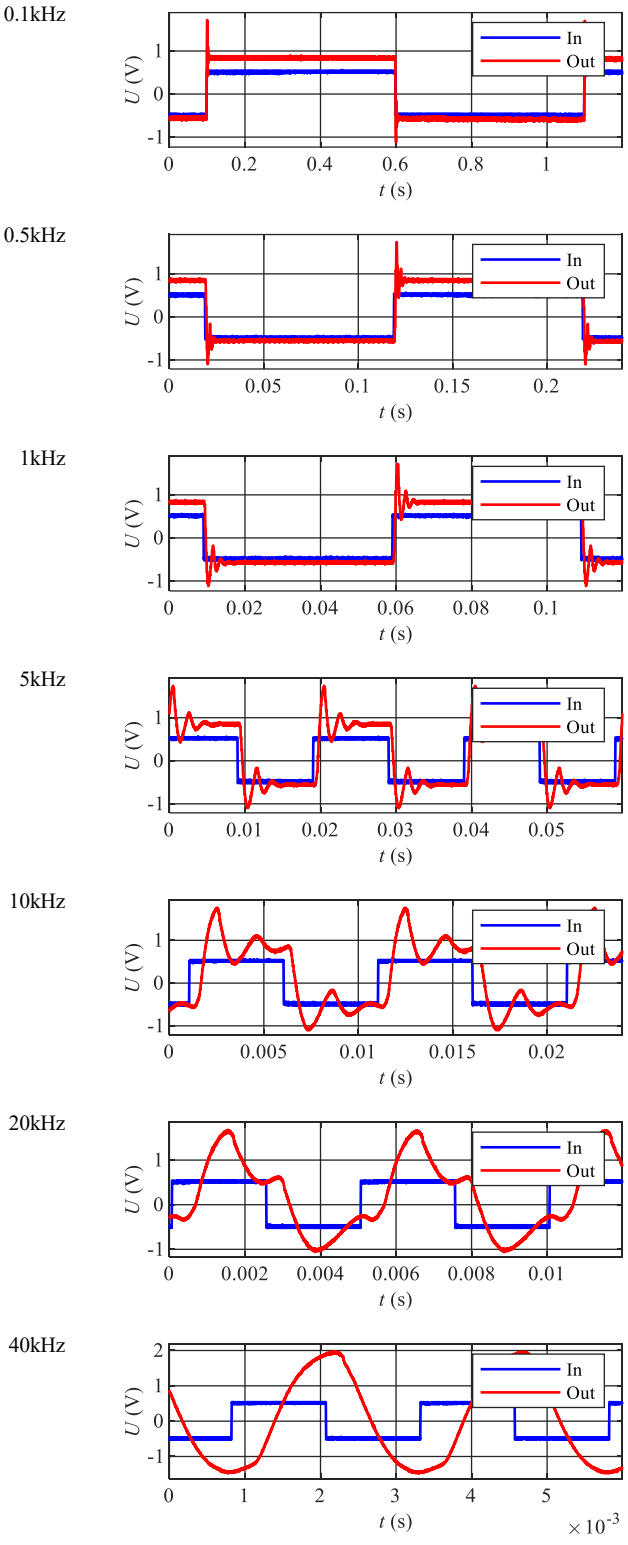

Figure 6. Measured power driver output without load with response to square wave input in a range of 100Hz to 40kHz.at

V. IDENTIFICATION WITH DS3031A LOAD

The next stage of the research included the use of a regulated load to diagnose the controller's operation at a load set to 1.7Ω. The voltage at the output of the controller's power system was measured. It should be emphasized that due to the load limitation of DL3031A only the unipolar signal was tested. The photo of the test bench is shown in Figure 7, and the connection diagram in Figure 8.

Figure 7. Programmable Automation Controller and laboratory equipement dedicated to hardware investigation.

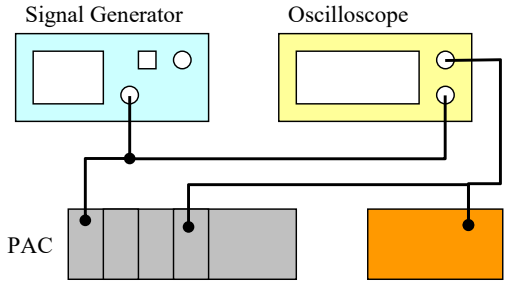

Figure 8. Schematic diagram of the PAC investigation with load.

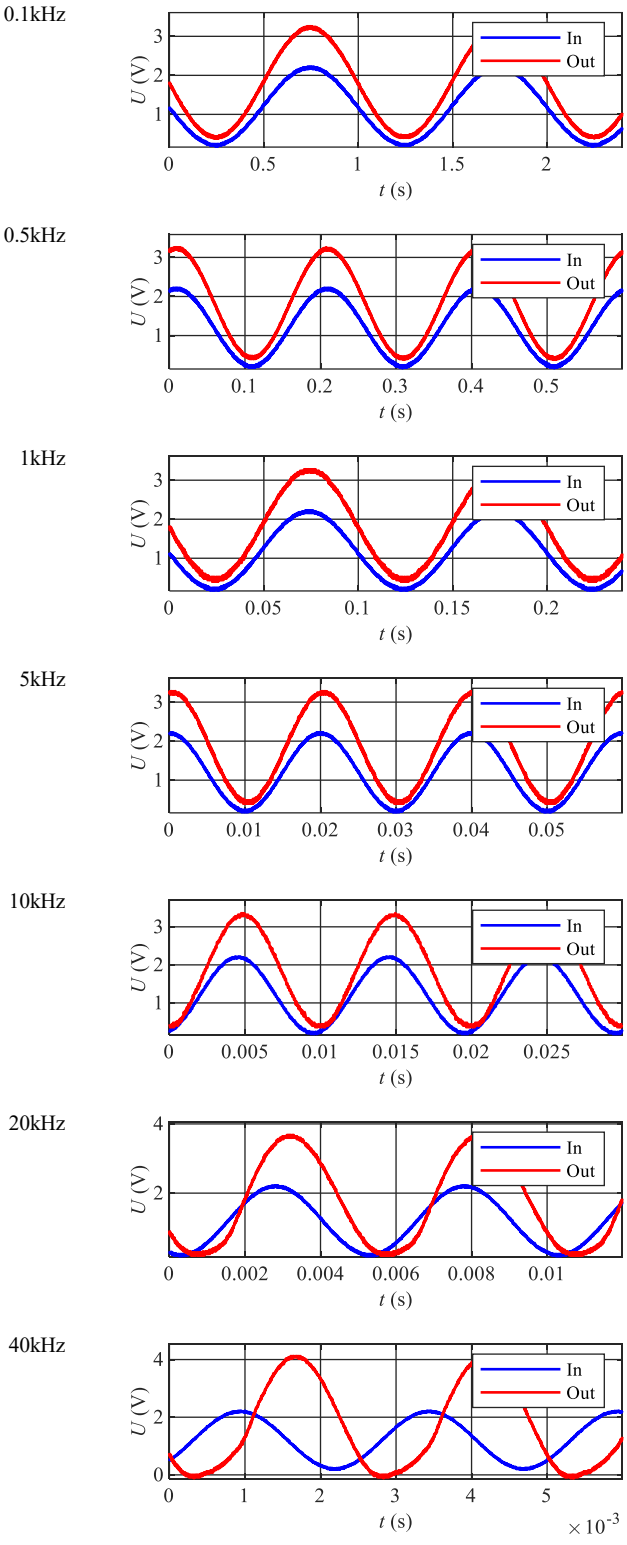

Figure 9. Measured power driver output with load with response to sine wve input in a range of 100Hz to 40kHz.

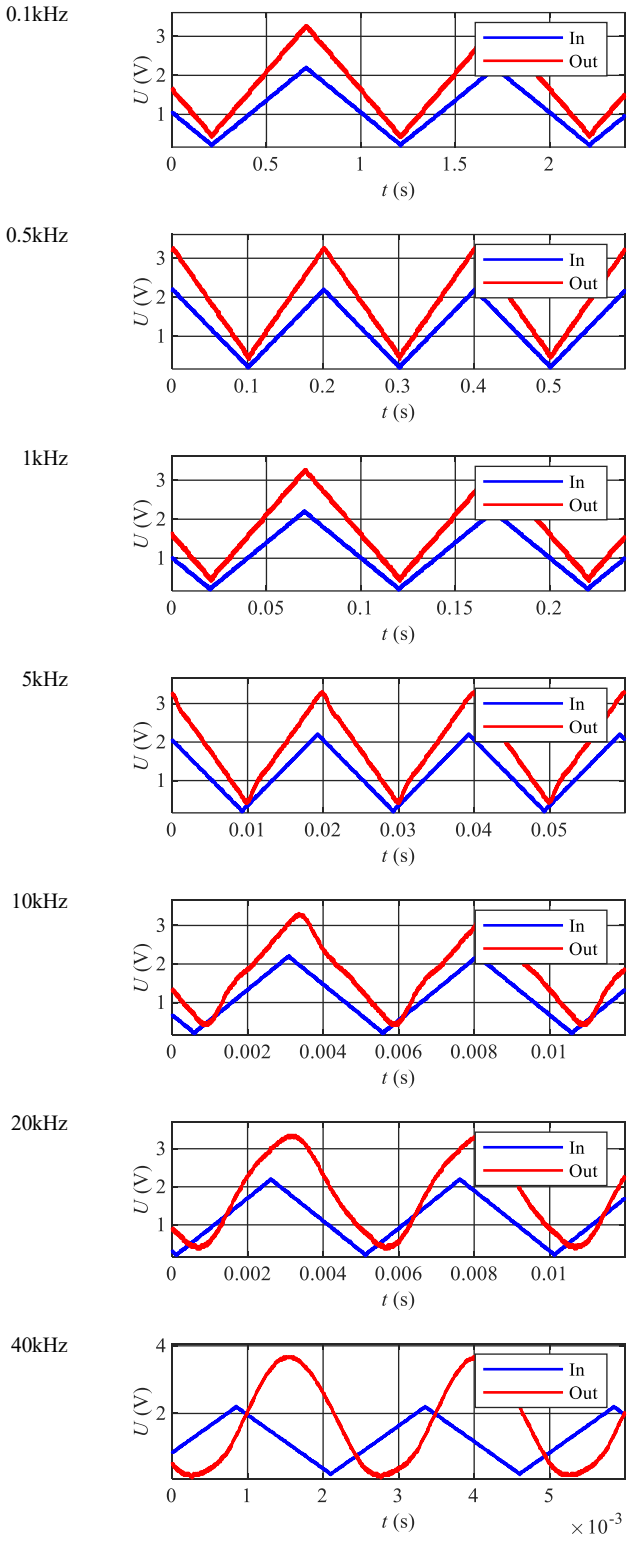

Figure 10. Measured power driver output with load with response to ramp wave input in a range of 100Hz to 40kHz.

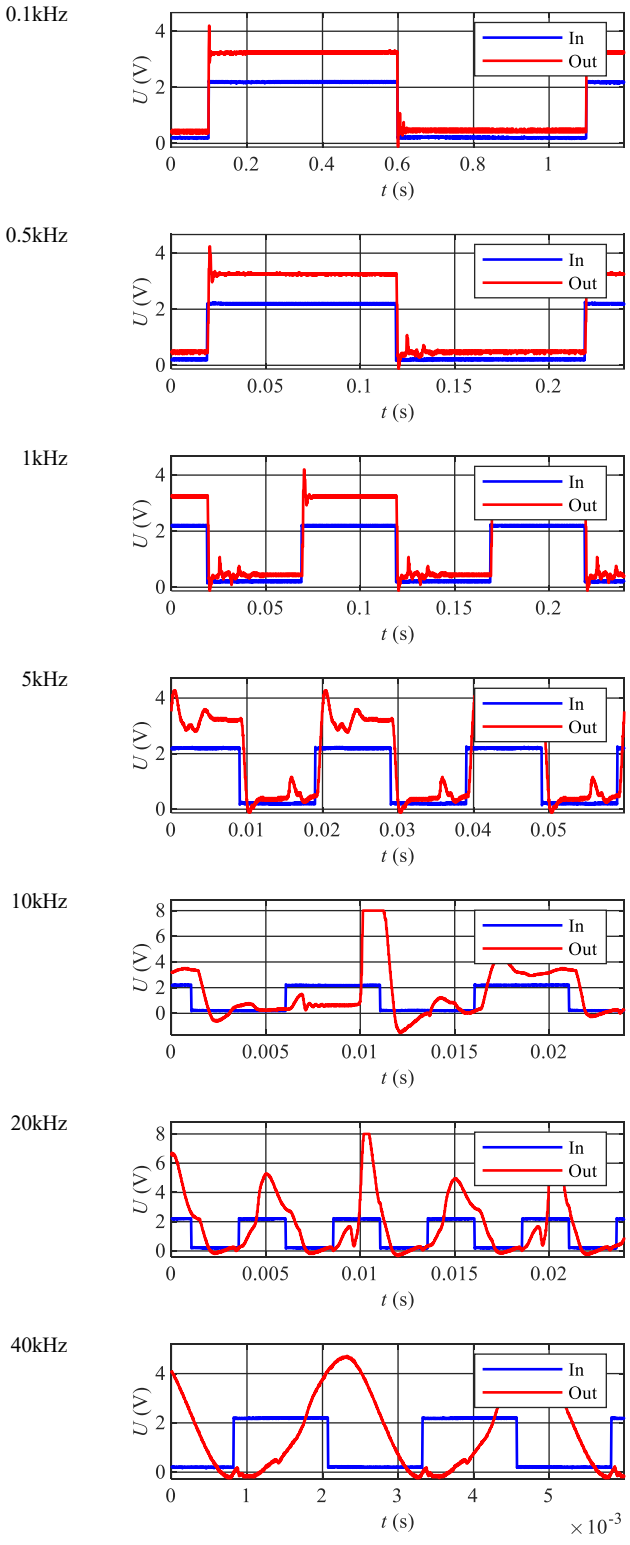

Figure 11. Measured power driver output with load with response to square wave input in a range of 100Hz to 40kHz.

The use of electronic load has allowed to study the characteristics at a resistive load (Figs. 9÷11). They confirmed good device performance up to 10kHz, although artifacts related to load coexistence were observed. The study showed changes in amplitude and phase shift.

VI. Identification with AMB

In the next study, a magnetic bearing with 4 actuators (Fig. 13) was used and the tests were repeated as in the open system. This time, the bipolar character of the power amplifier operation was used. The wiring diagram is shown in Figure 12.

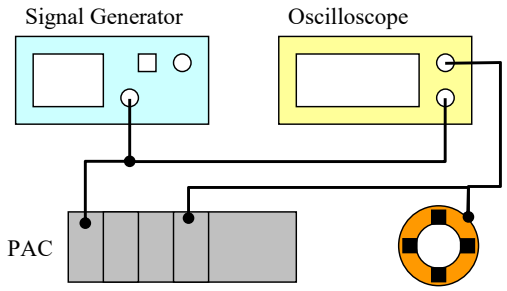

Figure 12. Schematic diagram of the PAC investigation with AMB connected to power module.

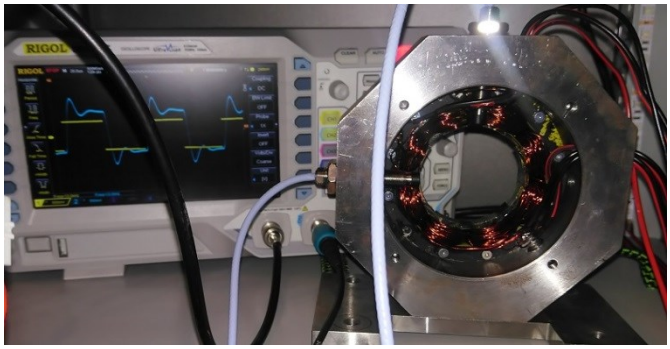

Figure 13. Active Magnetic Bearing at test-bench.

The results (Figs. 14÷16) obtained with the magnetic bearing confirm the good cooperation of the controller with an inductive element. It should be emphasized that in the whole frequency band there are no visible distortions in the case of a sinusoidal signal. It can be concluded that the test results for triangular and rectangular signals are satisfactory even up to 20kHz. On the basis of tests using a sinusoidal signal, the Bode characteristics were elaborated, which are illustrated in the examined frequency range in Figure 17. In the case of higher frequencies, the feedback of the power amplifier is insufficient and it will be necessary to modify the power system.

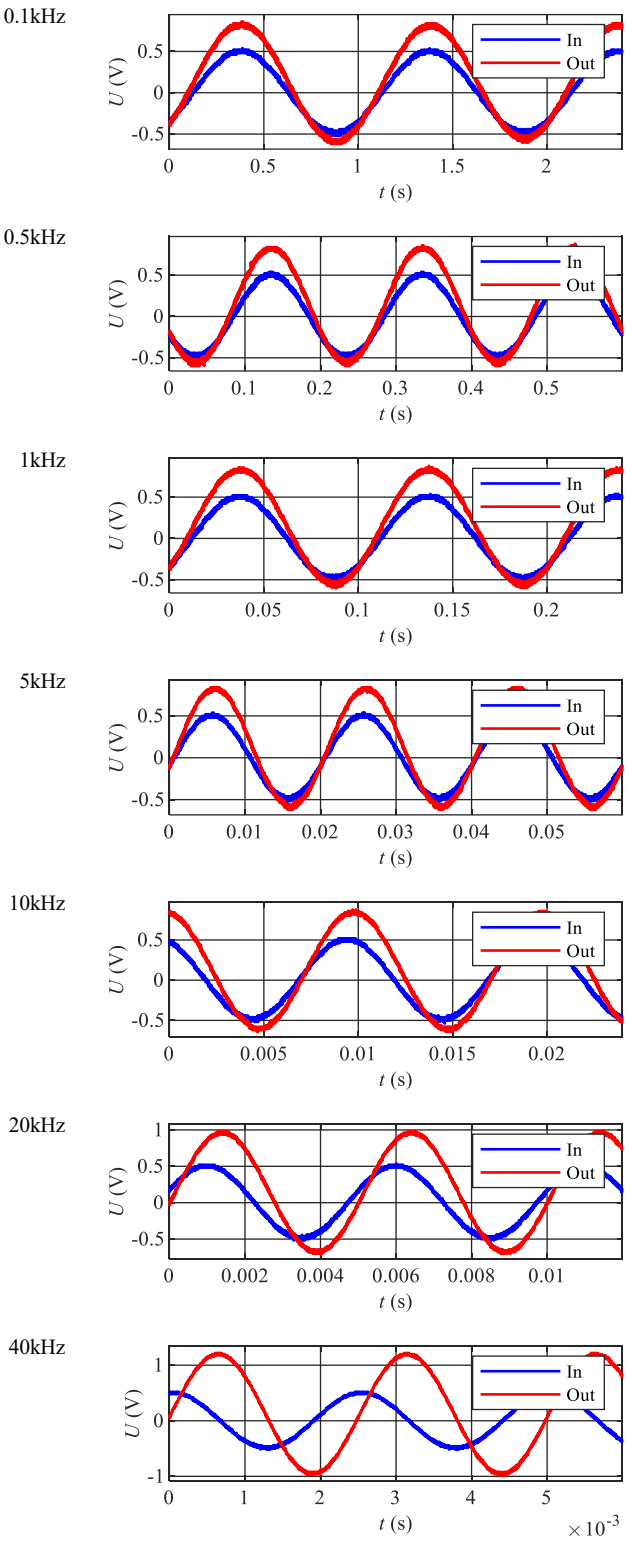

Figure 14. Measured power driver output with AMB load with response to sine wve input in a range of 100Hz to 40kHz.

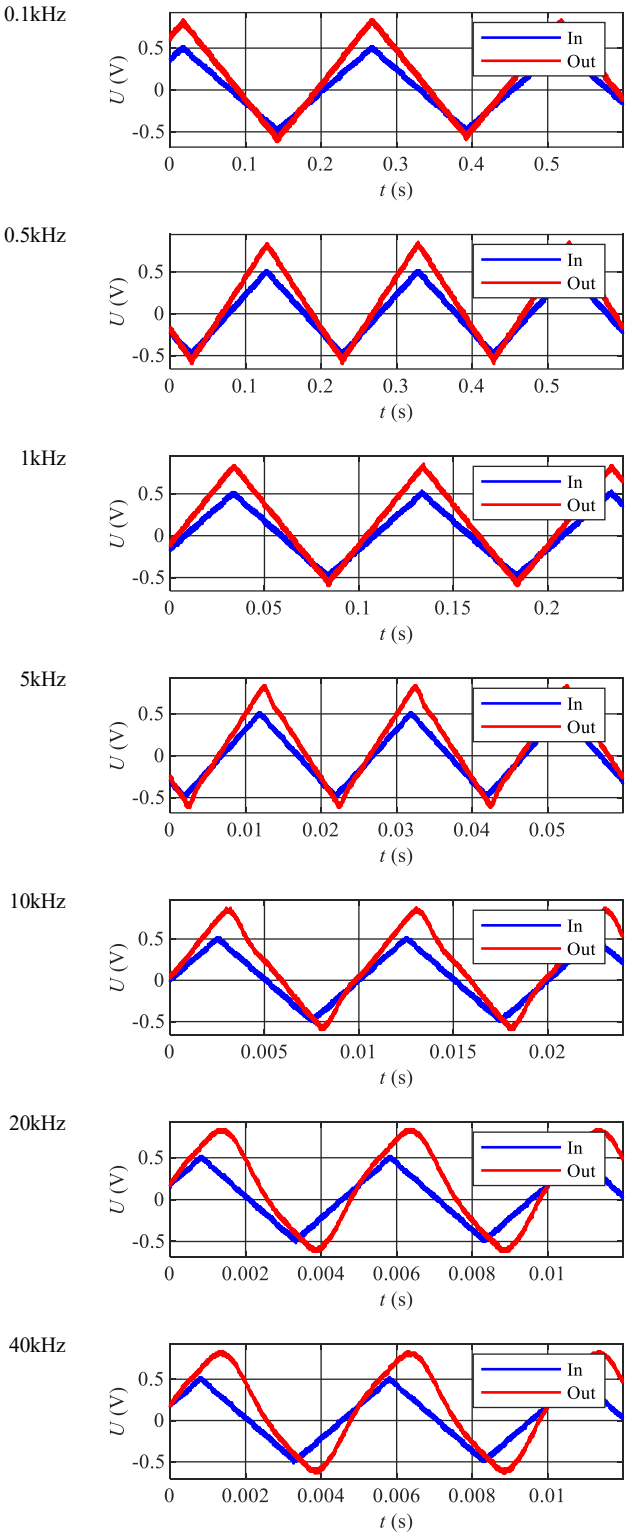

Figure 15. Measured power driver output with AMB load with response to ramp wave input in a range of 100Hz to 40kHz.

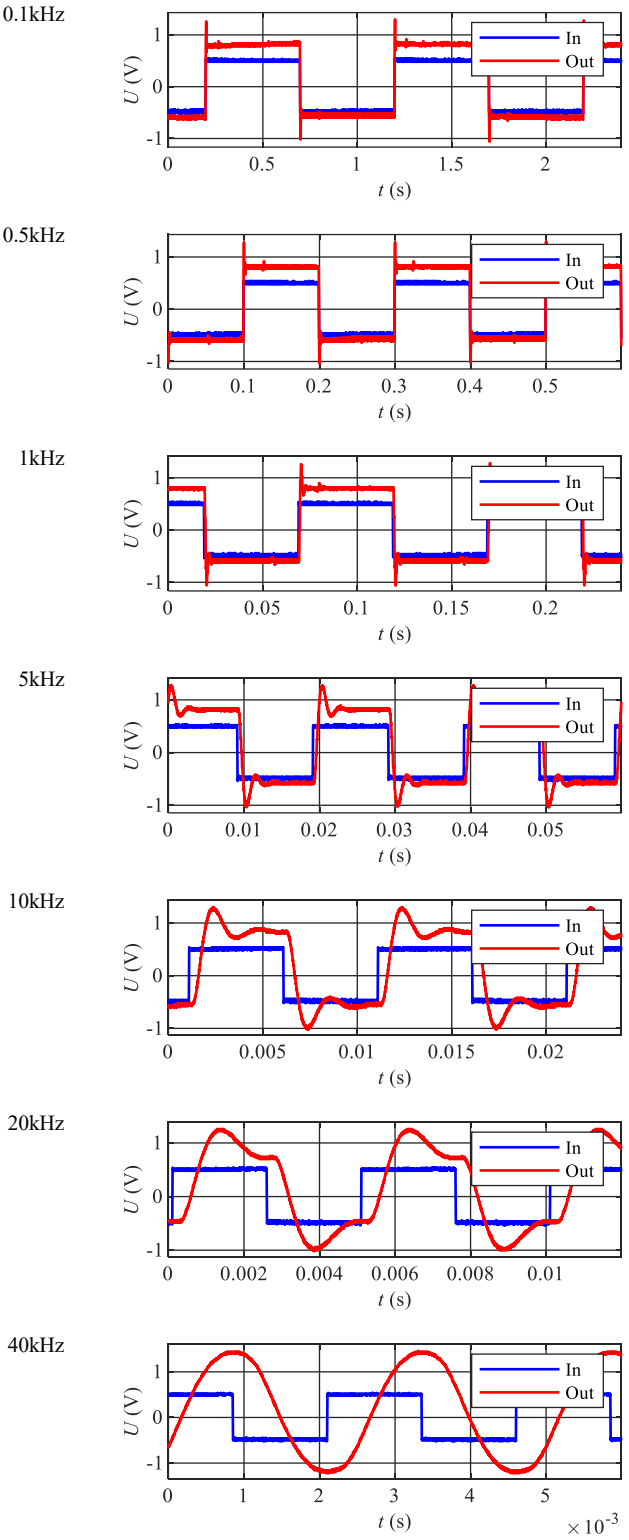

Figure 16. Measured power driver output with AMB load with response to square wave input in a range of 100Hz to 40kHz.

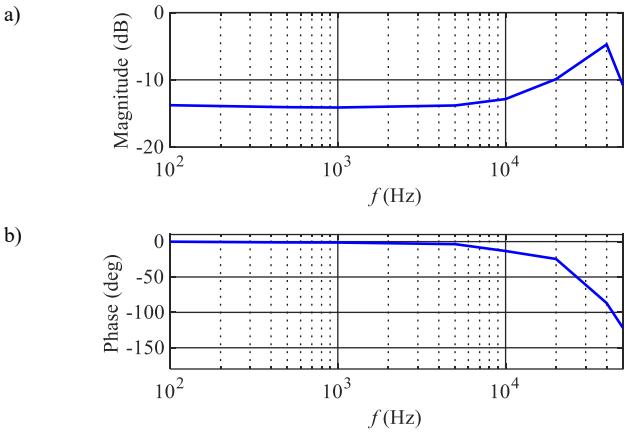

Figure 17. Magnitude (a) and phase (b) with respect to the frequence in the measured range obtained from experimental investigation of PAC with AMB load.

VII. Identification with AMB and Current Feedback

The last test was carried out using the internal feedback loop implemented in the PAC [18]. Its task was to regulate the current flowing through the power module with load. The wiring diagram is shown in Figure 18. It should be emphasized that from the point of view of the controller, the input signal generated by the signal generator becomes the set-point of the current. The internal regulator controls the power module in a proportional manner to obtain the desired current value at the load. This test was carried out using a magnetic bearing, because the application of load DL3031 disrupted the regulator due to its bipolar control action. When analyzing the test results, particular attention should be paid to the interpretation of signals: the input signal is the voltage corresponding to the current intensity set point, and the output signal is the voltage measured at the terminals of the electromagnetic actuator winding - analogically to previous tests.

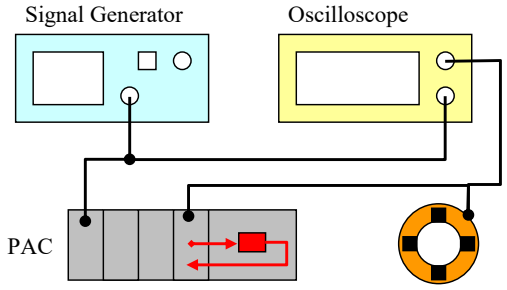

Figure 18. Schematic diagram of the PAC investigation with AMB connected to power module with internal current controller.

The regulator's operation is visible (see Figs. 19÷21). Unfortunately, the measurement of the coil supply voltage makes it difficult to analyze the results, however, it can be seen that the controller minimizes the error. It can be seen that the regulator minimizes the phase shift in the range up to 10kHz. Proportional feedback implemented every 1.5625µs improves operation, while the use of a different controller with a highly complex structure will be required.

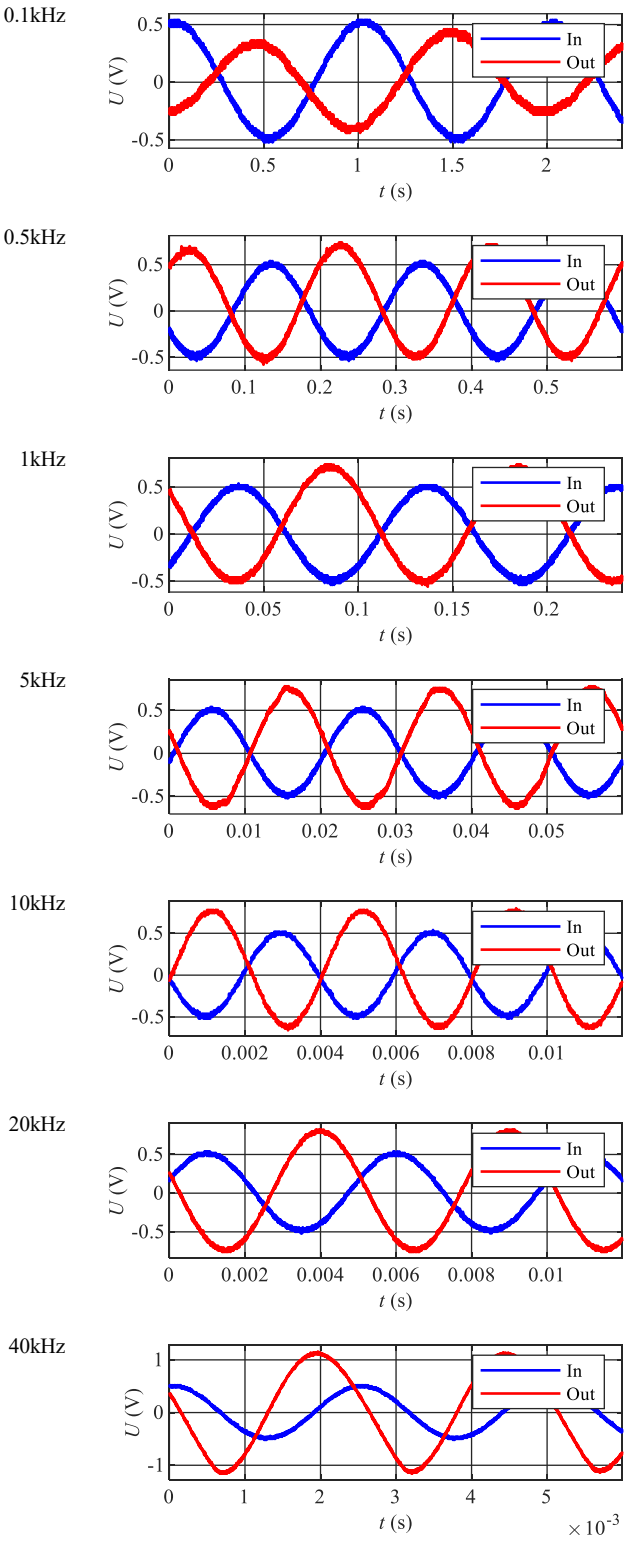

Figure 19. Measured power driver output with embedded controller under AMB load with response to sine wave input in a range of 100Hz to 40kHz.

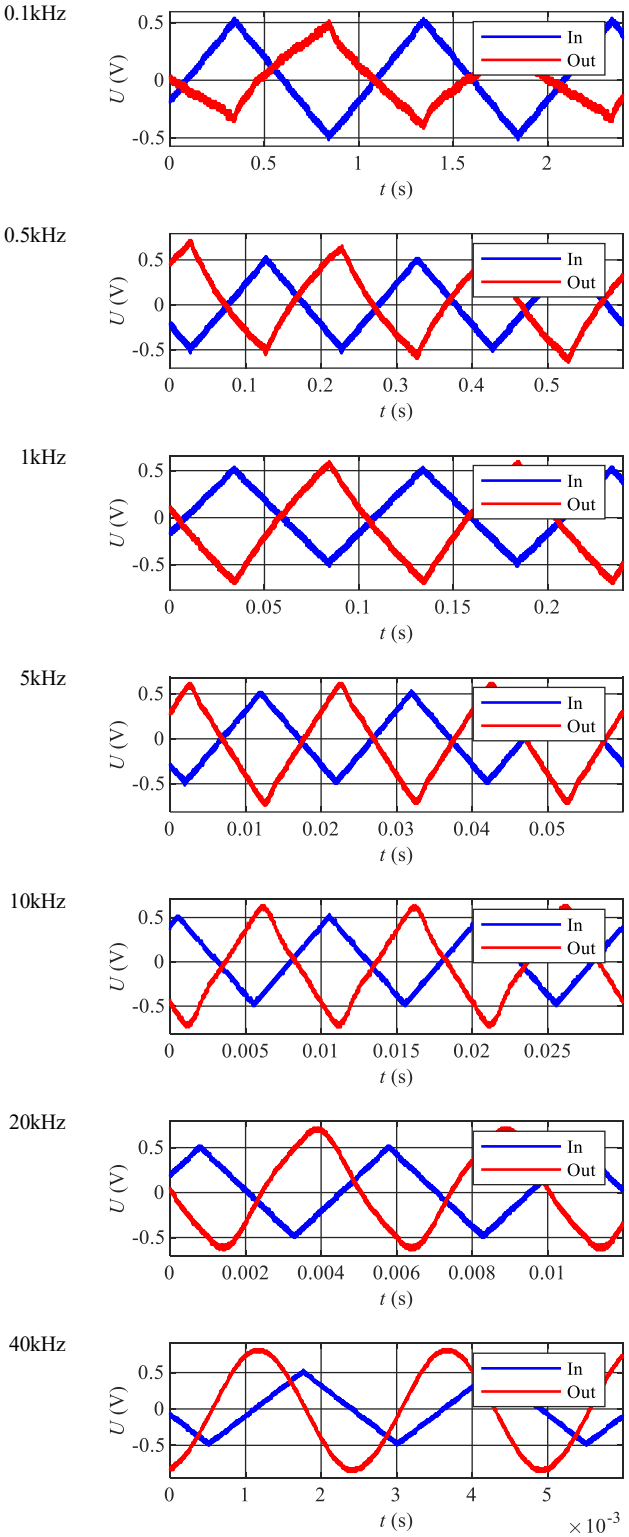

Figure 20. Measured power driver output with embedded controller under AMB load with response to ramp wave input in a range of 100Hz to 40kHz.

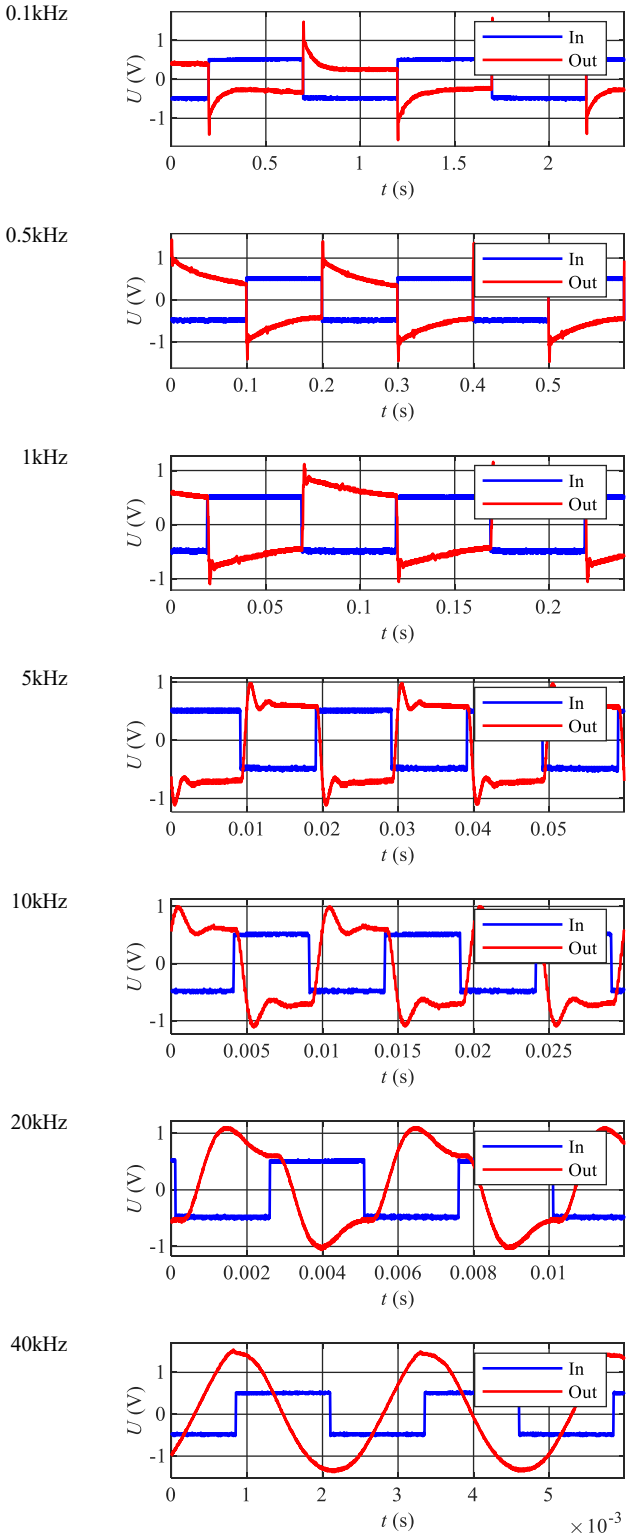

Figure 21. Measured power driver output with embedded controller under AMB load with response to square wave input in a range of 100Hz to 40kHz.

VIII. CONCLUSIONS

The presented results illustrate the operation of the controller's power system. They are particularly valuable, as technical documentation rarely presents time characteristics. The tests showed how the controller works with selected loads. The power system works correctly at the control values set. However, in the case of dynamic changes, its operation depends on the amplitude, load and type of control. Further research work should include broadening the bandwidth by modernizing the feedback loop in the analog power stage. Incorporation of the configured feedback has brought the expected results, while it is reasonable to conduct further research to expand the band width of the controller's power system with the use of a current regulator.

ACKNOWLEDGMENTS

This research was sponsored by ”Incubator of Innovation +”: project co-financed by the Ministry of Science and Higher Education under the program ”Support for management of scientific research and commercialization of BR results in scientific units and enterprises” under the Intelligent Development Operational Program 2014-2020.

REFERENCES

[1] Blödt M., Granjon P., Raison B., Rostaing G., Models for Bearing Damage Detection in Induction Motors Using Stator Current Monitoring. IEEE Transactions on Industrial Electronics. 2008, Vol. 55. No. 4, s. 1813–1822

[2] Chiba A., Fukao T., Ichikava O., Oshima M., Takemoto M., Dorrel D.G., Magnetic Bearings and Bearingless Drives. 2005, Newnes

[3] Despotovic Z.V., Stojiljkovic Z., Power Converter Control Circuits for Two-Mass Vibratory Conveying System With Electromagnetic Drive: Simulations and Experimental Results. IEEE Transactions on Industrial Electronics. 2007. Vol. 54. No. 1, s. 453–466

[4] Fang, J. Ren, Y., High-Precision Control for a Single Gimbal Magnetically Suspended Control Moment Gyro Based on Inverse System Method. IEEE Transactions on Industrial Electronics. 2011, Vol. 58. No. 9, s. 4331–4342

[5] Gosiewski Z., Magnetic bearings for rotational machinery, Theoretical aspects (In Polish). Wyższa Szkoła Inżynierska, 1993, Koszalin

[6] Gosiewski Z., Falkowski K., Multifunctional magnetic bearings (In Polish), BNIL, 2003, Warszawa

[7] Gosiewski Z., Kulesza Z., The use of FPGA systems to control magnetic bearing (In Polish),. 2007, Automaticon, Warszawa

[8] ISO 14839 Mechanical vibration – Vibration of rotating machinery equipped with active magnetic bearings, ISO 2012

[9] Jastrzębski R., Design and Implementation of FPGA-based LQ Control of Active Magnetic Bearings. 2007, PhD thesis, LUT, Finland

[10] Koch U., Wiedemann D., Ulbrich H. 2011: Model-Based MIMO State-Space Control of a Car Vibration Test Rig with Four Electromagnetic Actuators for the Tracking of Road Measurements. IEEE Transactions on Industrial Electronics. Vol. 58. No. 12, s. 5319–5323

[11] Kozanecka D. Digitally controlled magnetic bearing (In Polish), 2000, Zeszyty Naukowe Politechniki Łódzkiej, Łódź

[12] Krautz P., Nussbaumer T., Gruber W., Kolar J. W., Acceleration-Performance Optimization for Motors With Large Air Gap. IEEE Transactions on Industrial Electronics. 2010, Vol. 57. No. 1, s. 52–60Maslen, E. 1995: Magnetic Bearings. University of Virginia, Department of Mechanical, Aerospace and Nuclear Engineering, Charlottesville, Virginia.

[13] Maslen, E. 1995: Magnetic Bearings. University of Virginia, Department of Mechanical, Aerospace and Nuclear Engineering, Charlottesville, Virginia.

[14] Mukhopadhyay S. C., Ohji T., Iwahara M, Yamada S., Modeling and Control of a New Horizontal-Shaft Hybrid-Type Magnetic Bearing. 2000, IEEE Transactions on Industrial Electronics. Vol. 47. No. 1, s. 100–108

[15] Okhrimenko V. L., Shurubkin V. D., Magnetic suspension with a tuned circuit. 1976, Izmeritelnaya Tekhnika. October, No. 10, s. 89-90

[16] Piłat A., The programmable analog controller: static and dynamic configuration, as exemplified for active magnetic levitation. 2012, Przegląd Elektrotechniczny. ISSN 0033-2097. R. 88 nr 4b, s. 282–287

[17] Piłat A., Klocek J., Programmable Analog Hard Real-Time Controller. 2013, Przegląd Elektrotechniczny. ISSN 0033-2097. R. 89, nr. 3a/2013, s. 1–9

[18] Piłat A., Coil current proportional feedback embedded into programmable analog controller. 18th international conference on Methods and Models in Automation and Robotics, 26–29 August 2013, ISBN 978-1-4673-5506-3, Międzyzdroje, Poland

[19] Piłat A., Features and limitation of the programmable analogue signal processing for levitated devices. ISMB 12: proceedings of the twelfth International Symposium on Magnetic Bearings: August 22–25, 2010, Wuhan, China. Wuhan University of Technology Press, ISBN 978-7-900503-06-0, s. 482–489

[20] Piłat A., Testing performance and reliability of magnetic suspension controllers. MMAR 2009: 14th international conference on Methods and Models in Automation and Robotics: 19–21 August, 2009, Międzyzdroje, Poland, ISSN 1474-6670, www.ifac-papersonline.net, DOI: 10.3182/20090819-3-PL-3002.00029, s. 1–4

[21] Sawicki J.T., Maslen E.H., Bischof K.R., Modeling and Performance Evaluation of a Machining Spindle with Active Magnetic Bearings. KSME Journal of Mechanical Science and Technology. 2007, Vol. 21. No. 6, s. 847–850

[22] Schweitzer G., Traxler A., Bleurer H., Magnetlager, 1993 Springer Verlag, Heidelberg

[23] Schweitzer G., Maslen E. H., Bleuler H., Cole M., Keogh P., Larsonneur R., Nordmann R., Okada Y., Traxler A., Magnetic Bearings: Theory, Design, and Application to Rotating Machinery. 2009, Springer

[24] Williams R.D., Keith F.J., Allaire P.E., Digital Control of Active Magnetic Bearings. IEEE Transactions on Industrial Electronics. 1990, Vol. 31. No. 1, s. 19–27

[25] Yang, S.,Electromagnetic Actuator Implementation and Control for Resonance Vibration Reduction in Miniature Magnetically Levitated Rotating Machines. IEEE Trans. on Industrial Electronics, 2011, Vol. 58, No. 2, s. 611–617

[26] Yang Z.J., Kunitoshi K., Kanae S., Wada K., Adaptive Robust Output-Feedback Control of a Magnetic Levitation System by K-Filter Approach, IEEE Transactions on Industrial Electronics. 2008, Vol. 55. No. 1, s. 390–399